Bouncing cosmologies in the presence of a Dirac-Born-Infeld field

Mariam Campbell,[1] Richard Daniel,[2] Peter Dunsby,[1,3,4] and Carsten van de Bruck[2]
[1]*Department of Mathematics and Applied Mathematics, Cosmology and Gravity Group, University of Cape Town, Rondebosch, 7701, Cape Town, South Africa*
[2]*School of Mathematics and Statistics, University of Sheffield, Hounsfield Road, Sheffield S3 7RH, United Kingdom*
[3]*South African Astronomical Observatory, Observatory 7925, Cape Town, South Africa*
[4]*Centre for Space Research, North-West University, Potchefstroom 2520, South Africa*

(Received 20 June 2024; accepted 28 June 2024; published 5 August 2024)

We perform a detailed dynamical system analysis for the behavior of a Dirac-Born-Infeld (DBI) field in a spatially closed Friedmann-Lemaître-Robertson-Walker (FLRW) cosmology. The DBI field is characterized by a potential and brane tension. We study power-law or exponential functions for the potential and tension. We find that in a spatially closed FLRW cosmology, a DBI field in the ultrarelativistic limit allows for a broader range of initial conditions resulting in a bouncing universe than in the nonrelativistic limit. We further note that the range of initial conditions allowing for a bounce is larger if we consider power-law functions for the potential and tension, compared to the exponential case. Our dynamical analysis shows that a DBI field does not exhibit stable cyclical behavior, including the case in which a negative cosmological constant is present.

DOI: 10.1103/PhysRevD.110.043505

I. INTRODUCTION

Scalar fields have been studied extensively in theories of particle physics and cosmology [1,2]. In the standard model (SM), the Higgs boson is the only fundamental scalar field, but extensions of the SM, such as string theory, predict a plethora of new fundamental scalar fields [3,4]. In cosmology, they play an important role in models for the early and late time universe [5,6]. According to inflationary cosmology, at least one scalar field has driven a period of accelerated expansion in the very early universe and in dynamical models of dark energy the present accelerated expansion of the universe is usually driven by a scalar field.

One interesting class of scalar fields, so-called Dirac-Born-Infeld (DBI) fields, is suggested by string theory. These fields do not possess canonical kinetic terms. They describe the motion of D-branes in a higher-dimensional warped internal space and their origin is geometrical [7]. Since D-branes are described by DBI actions, it is not surprising that their kinetic term in the low-energy effective theory is noncanonical. The particular form of the DBI's kinetic term in the Lagrangian imposes a speed restriction analogous to the Lorentz factor in special relatively [8,9].

DBI fields have mainly been studied in the context of inflationary cosmology as part of k inflation, inflation driven by a scalar field with a noncanonical kinetic term [10–12]. Not surprisingly, because of the noncanonical kinetic term, the predictions of DBI inflationary models are different from standard slow-roll inflation. DBI's inherent speed limit allows for inflation to occur with steeper potentials compared to that of standard slow-roll inflation [13–18]. This allows for potentials motivated by other fields of study that were ruled out otherwise, such as "stringy" potentials. However, this relativistic feature in single-field inflation amplifies non-Gaussianities compared to the standard slow-roll inflationary model. This amplification provides a possible way to constrain such models with cosmological experiments and pin down the properties and origins of an inflationary field [19–24].

DBI fields have also been studied in the context of models for dark energy. The noncanonical kinetic term introduces interesting features in late-time cosmology, such as obtaining a cosmological constant behavior without a false vacuum [25–28]. A dynamical system analysis indicates a scaling solution proven to be attractor [29–31]. However, it is found that the nontrivial solutions and critical points in the phase-space analysis are highly dependent on the Lorentz term, γ, being large.

In this paper we perform a detailed dynamical system analysis of DBI dark energy models and extend the work of the literature in several ways. First, we allow for a nonzero spatial curvature. This is motivated by some works claiming that current observational data still marginally allows for a closed universe [32–34]. Even a small curvature at the present can have implications for the future evolution of the universe. Second, we study the impact of a negative cosmological constant on the dynamics of the DBI scalar field. There are some recent works studying dark energy in the presence of a negative cosmological constant [35–37].

From a theoretical perspective, either a nonzero curvature or a negative cosmological constant opens up the possibility of a bouncing cosmology, which could lead to a cyclic universe. Therefore, the aim of our study is to determine whether the dynamics of a DBI field naturally favors a universe with possible cyclic behavior.

This paper is organized as follows: In Sec. II, we present the model and the autonomous set of equations for a dynamical analysis. In Sec. III, we analyze the stability of a model with a power-law potential and brane tension. We also analyze the stability of an exponential behavior in Sec. IV. We illustrate the stability of both of the models in Sec. V. We continue our analysis, examining bouncing scenarios in Sec. VI and the effect of adding a negative cosmological constant in Sec. VII. We summarize and conclude our paper in Sec. VIII.

II. THE DBI MODEL

We consider the following action that in addition to Einstein gravity and matter, includes a DBI field, ϕ:

$$\mathcal{S}=\int d^4x\sqrt{-g}\left[\frac{R}{2}-\frac{1}{f(\phi)}(\gamma^{-1}-1)-V(\phi)+\mathcal{L}_m\right]. \quad (1)$$

In this equation, $\mathcal{L}_m$ is the Lagrangian that encodes the matter sector, $f^{-1}(\phi)$ is the D3-brane tension, encoding geometrical properties of the bulk spacetime, and $\gamma^{-1}=\sqrt{1+fX}$, where $X=g^{\mu\nu}\partial_\mu\phi\partial_\mu\phi$ [8,9]. We will assume throughout this work that V and f are strictly positive. Adopting the Friedmann-Lemaître-Robertson-Walker metric to describe an isotropic and homogeneous universe, and in which $a(t)$ is the scale factor, t the cosmic time, and assuming a homogeneous field ϕ, the kinetic term becomes $X=-\dot{\phi}^2$ and therefore

$$\gamma^{-1}=\sqrt{1-f\dot{\phi}^2}, \quad (2)$$

which acts as a Lorentz factor, bounding $\gamma\geq 1$ and $f^{-1}\geq\dot{\phi}^2$, thereby limiting the speed of the scalar field. The equation of motion for ϕ is (as usual $H=\dot{a}/a$)

$$\ddot{\phi}+3H\gamma^{-2}\dot{\phi}+\frac{1}{2}f_\phi f^{-2}(1-3\gamma^{-2}+2\gamma^{-3})+\gamma^{-3}V_\phi=0, \quad (3)$$

and Einstein's equations lead to the Friedmann equation:

$$3H^2=\frac{\gamma^2}{\gamma+1}\dot{\phi}^2+V+\rho_m-3\frac{K}{a^2}, \quad (4)$$

where ρ_m is the energy density of additional forms such as matter or radiation, and K encodes the spatial curvature. We will study the case of a closed universe in this paper and set $K=1$ for the remainder of the work. It will also be useful to define the energy density and pressure of the DBI field:

$$\rho_\phi=\frac{\gamma^2\dot{\phi}^2}{\gamma+1}+V,$$
$$P_\phi=\frac{\gamma\dot{\phi}^2}{\gamma+1}-V, \quad (5)$$

and ρ_m and ρ_r are the energy density of matter and radiation, respectively.

In the limit where $\dot{\phi}^2\to f^{-1}$, $\gamma^{-1}\to 0$. In this limit, which we will dub as *ultrarelativistic*, we see from Eq. (3) that the acceleration of field is governed by the brane tension, which results in a deceleration in an expanding universe as explored by [8,9], with the Friedmann equation, Eq. (4) dominated by the velocity of the field. On the other hand, when $\gamma\to 1$, Eqs. (3) and (4) result in the equations of motion for a canonical scalar field.

To analyze the dynamics of the system, we define the variables:

$$x=\frac{\dot{\phi}}{\sqrt{3\bar{\gamma}(1+\bar{\gamma})}}\frac{1}{D},\quad y=\frac{\sqrt{V}}{\sqrt{3}D},\quad z=\frac{H}{D},\quad \Omega_m=\frac{\rho_m}{3D^2} \quad (6)$$

where

$$D=\sqrt{H^2+\frac{K}{a^2}},\qquad \bar{\gamma}=\gamma^{-1}. \quad (7)$$

Here, x encodes the kinetic energy of the system, y the potential energy, and Ω_m is the matter density parameter, which has an equation of state parameter, w_m. To make the phase compact, we adopted the variable $\bar{\gamma}$, which is bounded between $0\leq\bar{\gamma}\leq 1$. Furthermore, to ensure a compact phase space in a closed universe, we introduce another variable, z, such that the spatial curvature is encoded in the effective Hubble parameter, D. The Friedmann equation, Eq. (4), in terms of these variables is then $x^2+y^2+\Omega_m=1$, which we will refer to as the Friedmann constraint. The energy density of the scalar field can be determined from the Friedmann constraint or Eq. (5), resulting in the energy density and equation of state,

$$\Omega_\phi=x^2+y^2,\qquad w_\phi=\frac{\bar{\gamma}x^2-y^2}{x^2+y^2}, \quad (8)$$

respectively. We characterize the potential and brane tension by introducing new parameters,

$$\lambda=-\frac{V_\phi}{V},\qquad \mu=-\frac{f_\phi}{f}. \quad (9)$$

To ensure that the system remains closed, we introduce a new time variable, τ, defined by $\frac{d}{d\tau} = D^{-1}\frac{d}{dt}$. We denote the derivative with respect to τ with a prime. The equations of motion [Eqs. (3) and (4)] result in the following set of equations:

$$\bar{\gamma}' = \frac{\tilde{\gamma}(1-\bar{\gamma}^2)}{\sqrt{1+\tilde{\gamma}}}\left[3\sqrt{1+\tilde{\gamma}}z + \frac{\sqrt{3\tilde{\gamma}}}{x}(\mu x^2 - \lambda y^2)\right], \tag{10}$$

$$x' = \frac{1}{2}\sqrt{3\tilde{\gamma}(1+\tilde{\gamma})}\lambda y^2 + \frac{3}{2}xz[-(1+\tilde{\gamma}) + (x^2+y^2)(1+w_\phi) + \Omega_m(1+w_m)], \tag{11}$$

$$y' = -\frac{1}{2}\sqrt{3\tilde{\gamma}(1+\tilde{\gamma})}\lambda xy + \frac{3}{2}[(x^2+y^2)(1+w) + \Omega_m(1+w_m)]yz, \tag{12}$$

$$z' = (1-z^2)\left[1 - \frac{3}{2}(y^2+x^2)(1+w) - \frac{3}{2}\Omega_m(1+w_m)\right], \tag{13}$$

and for completeness,

$$\Omega_m' = -3z(1+w_m)\Omega_m + 3\Omega_m[(1+w)(x^2+y^2) + (1+w_m)\Omega_m], \tag{14}$$

as a consequence of the Friedmann constraint. Maintaining generality, we also include the rate of change of λ and μ,

$$\mu' = \left(1 - \frac{f_{\phi\phi}f}{f_\phi^2}\right)\mu^2\sqrt{3\bar{\gamma}(1+\bar{\gamma})}x, \tag{15}$$

$$\lambda' = \left(1 - \frac{V_{\phi\phi}V}{V_\phi^2}\right)\lambda^2\sqrt{3\bar{\gamma}(1+\bar{\gamma})}x. \tag{16}$$

Utilizing Eqs. (15) and (16), we can note that the autonomous system can describe a wide range of potentials and brane tension functions. If we are to consider an exponential model, as often explored in quintessence models, we note that the μ and λ become a constant, reducing the number of equations to be solved.

III. MODEL WITH POWER-LAW BEHAVIOR

Following the work of [29], we consider a power-law function for both the potential $V(\phi)$ and the brane tension $f(\phi)$, which are forced to be strictly positive,

$$V(\phi) = \sigma|\phi|^p, \qquad f(\phi) = \nu|\phi|^r, \tag{17}$$

where $(\sigma,\nu) > 0$, and p and r are power-law parameters to be set.

A. Autonomous system

When considering the power-law functions, we reparametrize the potential and brane tension such that

$$\Lambda = -\frac{V_\phi}{f^q V^{q+1}}, \qquad M = -\frac{f_\phi}{f^{q+1}V^q}, \tag{18}$$

where $q = -1/(p+r)$. For the power-law case we are studying here, both Λ and M are constant, which allows us to reduce the number of equations for the system. We note that the case $q = 0$ identifies a specific behavior that reduces to the exponential scenario explored later in Sec. IV. The variables Λ and M are related to λ and μ by

$$\lambda = \left[\frac{(1-\bar{\gamma})y^2}{\bar{\gamma}(1+\bar{\gamma})x^2}\right]^q\Lambda, \qquad \mu = \left[\frac{(1-\bar{\gamma})y^2}{\bar{\gamma}(1+\bar{\gamma})x^2}\right]^q M. \tag{19}$$

As μ and λ can be written in terms of x, y, and z, we can utilize Eq. (18) with the need only to solve for x', y', and z'. Equations (10)–(13) become

$$\bar{\gamma}' = \frac{\bar{\gamma}(1-\bar{\gamma}^2)}{\sqrt{\bar{\gamma}+1}}\left[\frac{\bar{\gamma}^{\frac{1}{2}-q}\sqrt{3}}{x}\left(\frac{(1-\bar{\gamma})y^2}{(\bar{\gamma}+1)x^2}\right)^q(Mx^2 - \Lambda y^2) + 3\sqrt{\bar{\gamma}+1}z\right], \tag{20}$$

$$x' = \frac{\sqrt{3}}{2}[\bar{\gamma}(\bar{\gamma}+1)]^{\frac{1}{2}-q}\left[\frac{(1-\bar{\gamma})y^2}{x^2}\right]^q\Lambda y^2 + \frac{3xz}{2}\left[(\bar{\gamma}+1)(x^2-1) + \Omega_m(1+w_m)\right], \tag{21}$$

$$y' = -\frac{\sqrt{3}}{2}[\bar{\gamma}(\bar{\gamma}+1)]^{\frac{1}{2}-q}\left[\frac{(1-\bar{\gamma})y^2}{x^2}\right]^q\Lambda xy + \frac{3}{2}yz\left[x^2(1+\bar{\gamma}) + \Omega_m(1+w_m)\right], \tag{22}$$

$$z' = (1-z^2)\left[1 - \frac{3}{2}x^2(\bar{\gamma}+1) - \frac{3}{2}\Omega_m(1+w_m)\right]. \tag{23}$$

B. Stability analysis

Equations (20)–(22) potentially contain a singular fixed point due to $\bar{\gamma}^{-1}$ and x^{-1} terms. Therefore, in order to examine the fixed points, we determine the fixed points for $\bar{\gamma}$,

$$\bar{\gamma} = 0,$$
$$\bar{\gamma} = 1,$$
$$\frac{\bar{\gamma}^{\frac{1}{2}-q}\sqrt{3}}{x}\left(\frac{(1-\bar{\gamma})y^2}{(\bar{\gamma}+1)x^2}\right)^q (Mx^2 - \Lambda y^2) + 3\sqrt{\bar{\gamma}+1}z = 0.$$

We also restrict ourselves to examining unambiguous fixed points (solutions that do not result in 0/0) at the background level. We then examine the range of fixed points for x, y, and z for each case, summarized in Table I.

1. Case I: $\bar{\gamma} = 0$

The fixed point $\bar{\gamma} = 0$ corresponds to an ultrarelativistic field, with $\gamma \to \infty$. Therefore, the fixed point is an asymptotic solution instead of a truly physical one. In the ultrarelativistic scenario, we find a condition on q, $q \leq 1/2$, such that Eqs. (20)–(22) remain physical, thus constraining the potentials and warp functions. The resulting set of equations becomes

$$x' = \frac{3xz}{2}[(x^2-1) + \Omega_m(1+w_m)], \tag{24}$$

$$y' = \frac{3}{2}yz[x^2 + \Omega_m(1+w_m)], \tag{25}$$

$$z' = (1-z^2)\left[1 - \frac{3}{2}x^2 - \frac{3}{2}\Omega_m(1+w_m)\right]. \tag{26}$$

TABLE I. Each of the physical fixed points with corresponding stability and conditions for existence, for the power-law potential case.

γ	x	y	z	Existence		Stability
0	$\pm\sqrt{\frac{2-3\Omega_m(1+w_m)}{3}}$	$\sqrt{\frac{1}{3}+\Omega_m w_m}$	0	$q \leq 1/2$ $\Omega_m(1+w_m) \leq 3/2$		Saddle
				$\Omega_m \in (0:1)$	$w_m \in (0:1)$	Fig. 1, P5
0	$\pm\sqrt{1-\Omega_m(1+w_m)}$	0	-1	$q \leq 1/2$, $\Omega_m w_m = 0$, $\Omega_m(1+w_m) \leq 1$		Stable
				$\Omega_m \in (0:1)$	$w_m \in (0:1)$	Fig. 1, P1
0	$\pm\sqrt{1-\Omega_m(1+w_m)}$	0	1	$q \leq 1/2, \Omega_m w_m = 0$, $\Omega_m(1+w_m) \leq 1$		Unstable
				$\Omega_m \in (0:1)$	$w_m \in (0:1)$	Fig. 1, P2
0	0	$\sqrt{1-\Omega_m(1+w_m)}$	-1	$q \leq 1/2, \Omega_m w_m = 0$, $\Omega_m(1+w_m) \leq 1$		Unstable
0	0	$\sqrt{1-\Omega_m(1+w_m)}$	1	$q \leq 1/2, \Omega_m w_m = 0$, $\Omega_m(1+w_m) \leq 1$		Stable
0	0	0	-1	$q \leq 1/2$, $\Omega_m = 1$	$w_m > 0$	Stable
					$w_m < 0$	Unstable
				$\Omega_m \in (0:1)$	$w_m \in (0:1)$	Fig. 1, P3
0	0	0	1	$q \leq 1/2$, $\Omega_m = 1$	$w_m > 0$	Unstable
					$w_m < 0$	Stable
				$\Omega_m \in (0:1)$	$w_m \in (0:1)$	Fig. 1, P4
1	$\pm\sqrt{\frac{2-3\Omega_m(1+w_m)}{6}}$	$\sqrt{\frac{4-3\Omega_m(1-w_m)}{6}}$	0	$q > 0 \in \mathbb{R}$, $\Omega_m(1+w_m) \leq 2/3$		Saddle
				$\Omega_m \in (0:1)$	$w_m \in (0:1)$	Fig. 1, P6
1	$\pm\frac{\sqrt{2-\Omega_m(1+w_m)}}{\sqrt{2}}$	0	-1	$q > 0, \Omega_m(1-w_m) = 0, \Omega_m(1+w_m) \leq 2$		Stable
1	$\pm\frac{\sqrt{2-\Omega_m(1+w_m)}}{\sqrt{2}}$	0	1	$q > 0, \Omega_m(1-w_m) = 0, \Omega_m(1+w_m) \leq 2$		Unstable
1	0	$\sqrt{1-\Omega_m}$	1	$q > 0, w_m = -1$		Stable
1	0	$\sqrt{1-\Omega_m}$	-1	$q > 0, w_m = -1$		Unstable
1	0	0	-1	$q > 0$, $\Omega_m = 1$	$w_m = 1$	Stable
					$\lvert w_m\rvert < 1$	Saddle
					$w_m = -1$	Unstable
1	0	0	1	$q > 0$, $\Omega_m = 1$	$w_m = 1$	Stable
					$\lvert w_m\rvert < 1$	Saddle
					$w_m = -1$	Unstable
$\frac{1+3w_m\Omega_m}{3(\Omega_m-1)}$	$\pm\sqrt{1-\Omega_m}$	0	0	$q > 0, w_m < 0, \Omega_m > \frac{1}{3}, \frac{2}{3} > \Omega_m(1+w_m)$		Unstable
$\frac{3-\Lambda^2(1-\Omega)}{3}$	0	$\sqrt{1-\Omega_m}$	± 1	$q = -\frac{1}{2}, \Lambda^2(1-\Omega_m) < 3$		Unstable

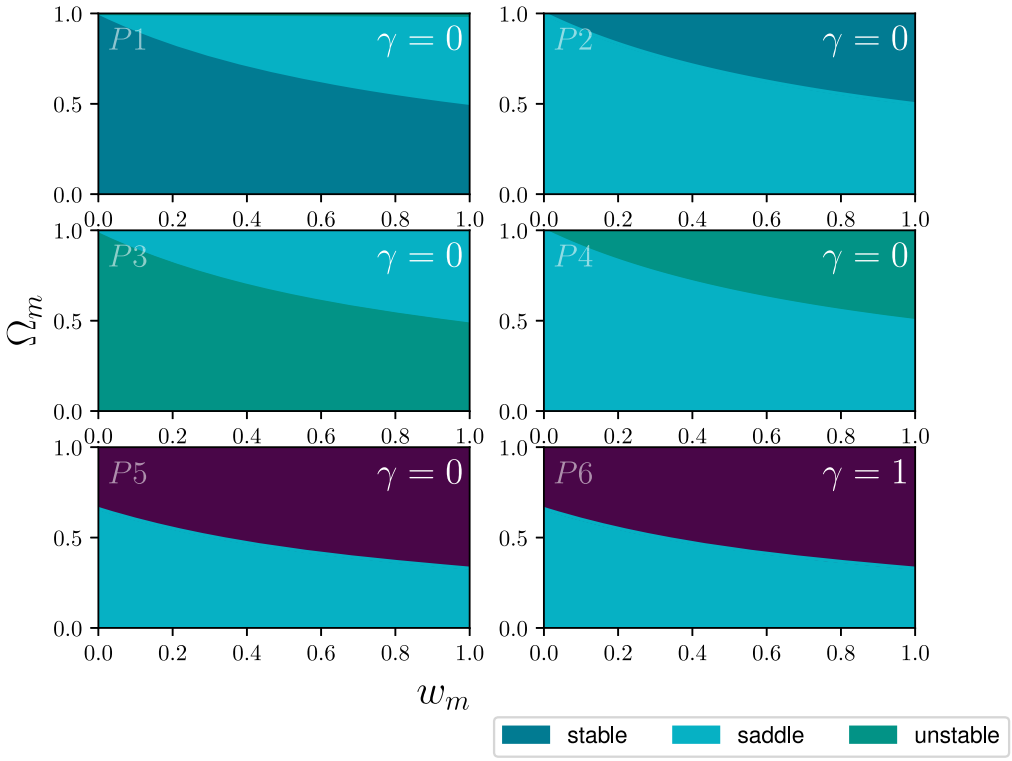

FIG. 1. Stability of fixed points for the power-law potential case, with $q = \frac{1}{2}$, as referenced in Table I. The purple regions in P5 and P6 correspond to a pair of parameter values that result in an imaginary fixed point.

In this case, the equations are now void of the parameter q, where the condition $q \leq 1/2$ has to be satisfied so that the system remains physical. We also note, given this condition, the equations are independent of the variable M and Λ, and thus on the specific choice of V and f.

Figure 1, panels P1–P5, describes the stability of the ultrarelativistic case for fixed points indicating expansion, contraction, and at the bounce. Panels P1 and P3 show the stability of the fixed points describing contraction, i.e., $z = -1$. When considering ultrastiff matter, $w_m = 1$, and $\Omega_m > 0.5$, we find the stability of these fixed points to be a saddle. When $w_m = 1/3$, radiation filled, and $\Omega < 0.7$, we see that the stability for P1 is stable and P3 is unstable.

Panels P2 and P4 show the stability of the fixed points describing expansion, i.e., $z = 1$. During expansion, we see that the stability of P2 is a swap of the stability of P1 and the stability of P4 is a swap of the stability of P3 for the matter cases considered.

Panel P5 describes the stability at the bounce, i.e., $z = 0$. We see that when $w_m = 1/3$, radiation filled, with $\Omega_m < 0.5$ the bounce has a saddle stability. Pressureless matter, $w_m = 0$, with $\Omega < 0.65$, shares the same stability. When considering ultrastiff matter, $w_m = 1$, and $\Omega_m > 0.3$, no real fixed points exist.

2. Case II: $\bar{\gamma} = 1$

In this scenario, provided $q \neq 0$, the dependence on γ is removed. In the case where $q = 0$, the system of equations reduces back to Eqs. (10)–(13). The $q = 0$ scenario is further explored in Sec. IV with the resulting fixed points given in Table II. Many fixed points will result in an ambiguity, i.e., terms that contain $0/0$, such as $x \to 0$. These are treated with care, and the nondivergent solutions are listed in Table I. The autonomous system is, for $q \neq 0$,

$$x' = \frac{3xz}{2}[2(x^2 - 1) + \Omega_m(1 + w_m)], \tag{27}$$

$$y' = \frac{3}{2}yz[2x^2 + \Omega_m(1 + w_m)], \tag{28}$$

$$z' = (1 - z^2)\left[1 - 3x^2 - \frac{3}{2}\Omega_m(1 + w_m)\right]. \tag{29}$$

It is worth noting that for $\bar{\gamma} = 1$ the DBI field behaves identically to the usual canonical scalar field. Interpreting $z > 0$ as a strictly expanding universe, the fixed points are $x = 1, y = 0, w_m = -1$, corresponding to the power-law inflationary fixed points [38]. Therefore, in later sections, we will compare the effects of including $\bar{\gamma} \neq 1$ against a canonical scalar field, $\bar{\gamma} = 1$.

We find that the ultrarelativistic and the canonical scalar have very similar resulting equations of motion, and as such similar behaving fixed points. For instance, in regards to z', the fixed point is determined by the kinetic energy, the value of x^2 as seen from Eq. (23). From Table I, we see that

TABLE II. Additional fixed points for $q = 0$, an exponential potential and brane tension.

$\bar{\gamma}$	x	y	z	Ω_m	Existence	Stability
1	-1	0	-1	0	$0 \leq w_m < 1$ and $0 \leq \lambda \leq \frac{6}{\sqrt{6}}$	Stable
					$0 \leq w_m \leq 1$ and $\lambda > \frac{6}{\sqrt{6}}$	Saddle
1	-1	0	1	0	$0 \leq w_m \leq 1$ and $\lambda > 0$	Unstable
1	0	0	-1	1	$0 \leq w_m < 1$ and $\lambda \in \mathbb{R}$	Saddle
					$w_m = 1$ and $\lambda \in \mathbb{R}$	Stable
1	0	0	1	1	$0 \leq w_m < 1$ and $\lambda \in \mathbb{R}$	Saddle
					$w_m = 1$ and $\lambda \in \mathbb{R}$	Unstable
1	1	0	-1	0	$0 \leq w_m \leq 1$ and $\lambda \in \mathbb{R}$	Stable
1	1	0	1	0	$0 \leq w_m \leq 1$ and $0 \leq \lambda < \frac{6}{\sqrt{6}}$	Unstable
1	$-\frac{1}{\sqrt{3}}$	$\sqrt{\frac{2}{3}}$	$-\frac{\lambda}{\sqrt{2}}$	0	$0 \leq w_m \leq 1$ and $\sqrt{\frac{6}{3}} < \lambda \leq \sqrt{\frac{8}{3}}$	Unstable
					$0 \leq w_m \leq 1$ and $0 < \lambda < \sqrt{2}$	Saddle
					$0 \leq w_m \leq 1$ and $\lambda > \sqrt{\frac{8}{3}}$	Unstable spiral
1	$\frac{1}{\sqrt{3}}$	$\sqrt{\frac{2}{3}}$	$\frac{\lambda}{\sqrt{2}}$	0	$0 \leq w_m \leq 1$ and $\sqrt{2} < \lambda \leq \sqrt{\frac{8}{3}}$	Stable
					$0 \leq w_m \leq 1$ and $0 < \lambda < \sqrt{2}$	Saddle
					$0 \leq w_m \leq 1$ and $\lambda > \sqrt{\frac{8}{3}}$	Unstable spiral

when the relative kinetic energy of our scalar field is not dominating, $x^2 \to 0$, we find the dynamics result in a quasi-de-sitter expansion. An expected result from a slow-rolling scalar field. However, with a fast-rolling scalar field, $x^2 \to 1$, the dynamics result in a singular collapse, identified as the "Big Crunch."

Figure 1, P6, shows the stability at the bounce, $z = 0$, for the specific case $q = 1/2$. The stability at the bounce is the same as in the ultrarelativistic case, $\bar{\gamma} = 0$, at the bounce.

3. Case III: $0 < \gamma < 1$

Here we further identify fixed points using $\frac{\bar{\gamma}^{\frac{1}{2}-q}\sqrt{3}}{x}\left(\frac{(1-\bar{\gamma})y^2}{(\bar{\gamma}+1)x^2}\right)^q(Mx^2 - \Lambda y^2) + 3\sqrt{\bar{\gamma}+1}z = 0$ where $\bar{\gamma}$ remains a constant between 0 and 1. Assuming that $q \neq 0$, we use the fixed point to remove the dependence on the q parameter by setting

$$\sqrt{3}[\bar{\gamma}(\bar{\gamma}+1)]^{\frac{1}{2}-q}\left[\frac{(1-\bar{\gamma})y^2}{x^2}\right]^q = \frac{3xz\sqrt{\bar{\gamma}+1}}{(\Lambda y^2 - Mx^2)}. \tag{30}$$

This allows us to remove the q dependency in Eqs. (21) and (22):

$$x' = \frac{3}{2}\left[\frac{\sqrt{\bar{\gamma}+1}}{(\Lambda y^2 - Mx^2)}\Lambda y^2 + (\bar{\gamma}+1)(x^2-1) + \Omega_m(1+w_m)\right]xz, \tag{31}$$

$$y' = \frac{3}{2}\left[-\frac{\sqrt{\bar{\gamma}+1}}{(\Lambda y^2 - Mx^2)}\Lambda x^2 + (1+\bar{\gamma})x^2 + \Omega_m(1+w_m)\right]yz, \tag{32}$$

with z' remaining unchanged. Upon analyzing the set of Eqs. (23), (31), and (32), we find that there are no stable fixed points for $0 < \bar{\gamma} < 1$, as identified in Table I. Regarding the resulting behavior of the system, we utilize the relationship between z' and x^2. If the kinetic energy is dominating in Eq. (23) such that $x^2(\bar{\gamma}+1) > \frac{2}{3} - \Omega_m(1+w_m)$, this drives z to negative values. On the other hand, if the kinetic energy is not dominating, $x^2(\bar{\gamma}+1) < \frac{2}{3} - \Omega_m(1+w_m)$, then z will be driven to positive values.

Furthermore, if we allow $\bar{\gamma}$ to evolve from Eq. (10), we can see that the resulting negative (positive) z, which is a product of large (small) values of x^2, drives $\bar{\gamma}$ towards zero (one) and consequently to the fixed points determined for $\bar{\gamma} = 0$ or $\bar{\gamma} = 1$. We interpret this result as the system being highly unstable in the regime of $0 < \bar{\gamma} < 1$, with the resulting stable fixed point highly dependent on the initial conditions given.

IV. MODEL WITH AN EXPONENTIAL POTENTIAL

Now we consider the case in which both the potential and brane tension depend exponentially on the scalar field,

$$V(\phi) = \sigma e^{-\lambda\phi}, \qquad f(\phi) = \nu e^{-\mu\phi}, \tag{33}$$

where σ, ν, μ, and λ are constants. This implies that Eqs. (15) and (16) are automatically set to zero. The power-law case in Sec. III can be related to an exponential function with ϕ in the limit $(p, r) \to \infty$. This reduces the following parameters to $q \to 0$ and $\Lambda \to \lambda$, $M \to \mu$. The resulting autonomous equations are given by Eqs. (10)–(13). In the limit $q = 0$, the autonomous system is described by Eqs. (20)–(23).

A. Stability analysis

Performing the same fixed point analysis as in Sec. III, we begin by determining the fixed points of Eq. (10), which has three roots:

$$\bar{\gamma} = 0,$$
$$\bar{\gamma} = 1,$$
$$\bar{\gamma} = \frac{3x^2z^2}{(\mu x^2 - \lambda y^2)^2 - 3x^2z^2}.$$

1. Case I: $\bar{\gamma} = 0$

Setting $q = 0$ for $\bar{\gamma} = 0$ results in the same set of autonomous equations as Eqs. (24)–(26). Therefore, the fixed points and their stability are the same in this case as given in Table I.

2. Case II: $\bar{\gamma} = 1$

Reemphasizing, as in Sec. III, $\bar{\gamma} = 1$ represents a canonical scalar field. For the case $q = 0$, the result is an exponential potential similar to that found in dark energy models [39]. The autonomous system reads

$$x' = \frac{3}{2}xz[2(x^2 - 1) + \Omega_m(1 + w_m)] + \sqrt{\frac{3}{2}}\lambda y^2, \tag{34}$$

$$y' = \frac{3yz}{2}[2x^2 + \Omega_m(1 + w_m)] - \sqrt{\frac{3}{2}}\lambda xy, \tag{35}$$

$$z' = (1 - z^2)\left[1 - 3x^2 - \frac{3}{2}\Omega_m(1 + w_m)\right]. \tag{36}$$

The fixed points' outcomes and characteristics are presented in Table II. The table shows that the fixed points exhibit behavior analogous to the power-law's description. Specifically, when the potential is zero ($y = 0$), the only stable fixed point corresponds to a collapse leading to a singular Big Crunch. However, including a nonzero potential ($y > 0$) results in the general behavior of the Universe, which tends toward a quasi-de-Sitter solution. This finding aligns with prior research in the field [39–41]. It tells us that the universe will eventually collapse without a scalar field i.e., no dark energy or a zero potential. However, it is important to acknowledge that these scenarios are physically unrealistic, as dictated by the inherent nature of exponential decay where $V > 0$, implying $y \neq 0$. The solution resembles standard quintessence with a nonzero potential, with dark energy dominating the dynamics.

3. Case III: $\bar{\gamma} = \frac{3x^2z^2}{-3x^2z^2 + (\mu x^2 - \lambda y^2)^2}$

The resulting fixed points specifying $\bar{\gamma} = \frac{3x^2z^2}{-3x^2z^2 + (\mu x^2 - \lambda y^2)^2}$ result in either $x = 0$ or $z = 0$. Therefore, $\bar{\gamma} = 0$, resulting in a repeated fixed point. Thus, the $q = 0$ case results in no new fixed points.

V. NUMERICAL ANALYSIS

We numerically analyze the system's behavior for the case $q = 1/2$ to indicate the behavior of the commonly cited scenario of $V \propto \phi^2$ and $f \propto \phi^{-4}$. We have numerically explored other values of q, with little difference in the overall dynamical behavior. We also note that the behavior of the potential, y, is not included in Figs. 2 and 3 as this provides little insight and is constrained by the Friedmann equation.

The fixed points resulting in $\bar{\gamma} = 0$ and $\bar{\gamma} = 1$ have similar behaviors, as illustrated in Fig. 2. We see the emergence of the stable solutions, identified in Table I, for $y, z = 0, -1$ and $x, z = 0,\ 1$, which correspond to an accelerated collapse or accelerated expansion, respectively. The saddle solution at $z = 0$ is also clearly depicted in Fig. 2, for $\bar{\gamma} = 0$ and $\bar{\gamma} = 1$, corresponding to the saddle found in Table I.

Although, there seems to be a resemblance of an almost unstable cyclic behavior at $z = 0, \bar{\gamma} = 1/2$, this is an artifact of the transition between $z < 0$ flowing towards $\bar{\gamma} \to 0$ and $z > 0$ flowing towards $\bar{\gamma} \to 1$. There is an unstable point at $z = 0$ while $0 < \bar{\gamma} < 1$ in Table I, but it is not well defined given the choice of parameters in Fig. 2. Expanding the cross section to examine further values of $\bar{\gamma}$ between 0 and 1, results in the same behavior as seen for $\bar{\gamma} = 1/2$. We conclude that the dynamics in the regime $1 > \bar{\gamma} > 0$ quickly result in an ultrarelativistic $\bar{\gamma} = 0$ or standard quintessence $\bar{\gamma} = 1$ scenario. Thus, the dynamics always result in a quasi-de-Sitter Universe, $z \to \pm 1$, as specified by stable solutions in Table I.

We also study the initial conditions and the time taken for the Universe to end up in the final solution of $z \to \pm 1$ as shown in Fig. 3, where the colors of the individual trajectories denote the initial value for the variable x. As it can be seen, trajectories in phase space are highly dependent on the initial conditions, which is similar to what happens in many models that include bouncing cosmologies. A universe is generally more likely to end up in an expanding Universe if it has a dominant kinetic energy and more likely to result in a collapse if the kinetic energy is subdominant. This effect can be seen in Fig. 3, where the

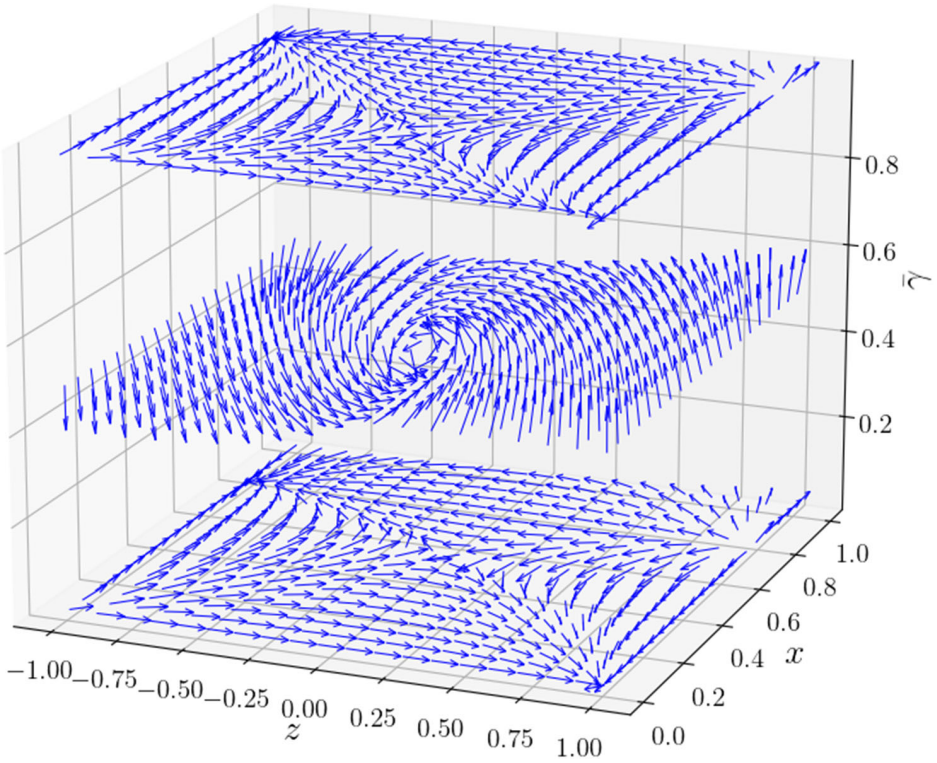

FIG. 2. A phase plot showing the behavior of the system with $q = 1/2$, $\Omega_m = 0.2$, $w_m = 1/3$, and $M = \Lambda = 10^{-4}$.

initial conditions of the kinetic term vary in values of $\bar{\gamma}$. In addition, there are unstable spiral solutions that exhibit a cyclic solution which quickly tend towards and singular collapse or quasi-de-Sitter Universe. However, these are not included in Fig. 3, due to the resolution and the exhaustive numerical analysis required to study these particular solutions.

An interesting result from our analysis is the enhancement of the phase space of a resulting bounce scenario ($z < 0 \to z > 0$) in ultrarelativistic scenarios compared to a canonical scalar field scenario. This feature is explored further in the next section.

VI. BOUNCING COSMOLOGIES WITH A DBI FIELD

We have concluded that stable, generic cyclic models are not exhibited in a DBI model. However, it was found that the "deceleration" mechanisms of the scalar field provide a more extensive range of initial conditions that lead to a bounce. This can be seen in Figs. 2 and 5 for the ultrarelativistic case ($\bar{\gamma} = 0$), compared to the standard quintessence case ($\bar{\gamma} = 1$).

We investigate this aspect further in the following. Provided a range of initial conditions for z_i, x_i, with the dependence on y_i determined by the Friedmann constraint, we numerically integrate the system as before for Fig. 3. This results in a relationship between the initial conditions and the dynamics, resulting in a bounce. This is shown in Fig. 4, in which the area under each graph shows the initial conditions that will result in a bounce.

In the case of an exponential form for potential and brane tension, for which the results are shown in Fig. 4, we find an increase of 69% in initial conditions for the ultrarelativistic case, $\bar{\gamma} = 0$, will lead to a bounce, whereas $\bar{\gamma} = 0.5$ leads to a 36% increase in initial conditions resulting in a bounce. For the power-law case with $q = 0.5$, we find that for the ultrarelativistic case, there is a 77% increase in the initial conditions that result in a bounce. This drops to a 41% increase at $\bar{\gamma} = 0.5$.

Note that smaller z_i values correspond to a slower contraction of the Universe, which results in more time for the spatial curvature to dominate and a larger range of x_i values that result in a bounce. We can see from Fig. 4 that including the DBI model with the condition $\bar{\gamma} < 1$, the range of initial conditions that lead to a bounce increases as the initial value of $\bar{\gamma}$ grows towards an ultrarelativistic state, $\bar{\gamma} = 0$.

VII. ADDING A NEGATIVE COSMOLOGICAL CONSTANT

As we have seen in the previous section, after the bounce the dynamics results in a quasi-de-Sitter expansion, $z \to +1$. In the following we include a negative cosmological constant to arrange for this system to recollapse. The aim of this analysis is to see whether the universe would, as a result, settle into a cyclic behavior.

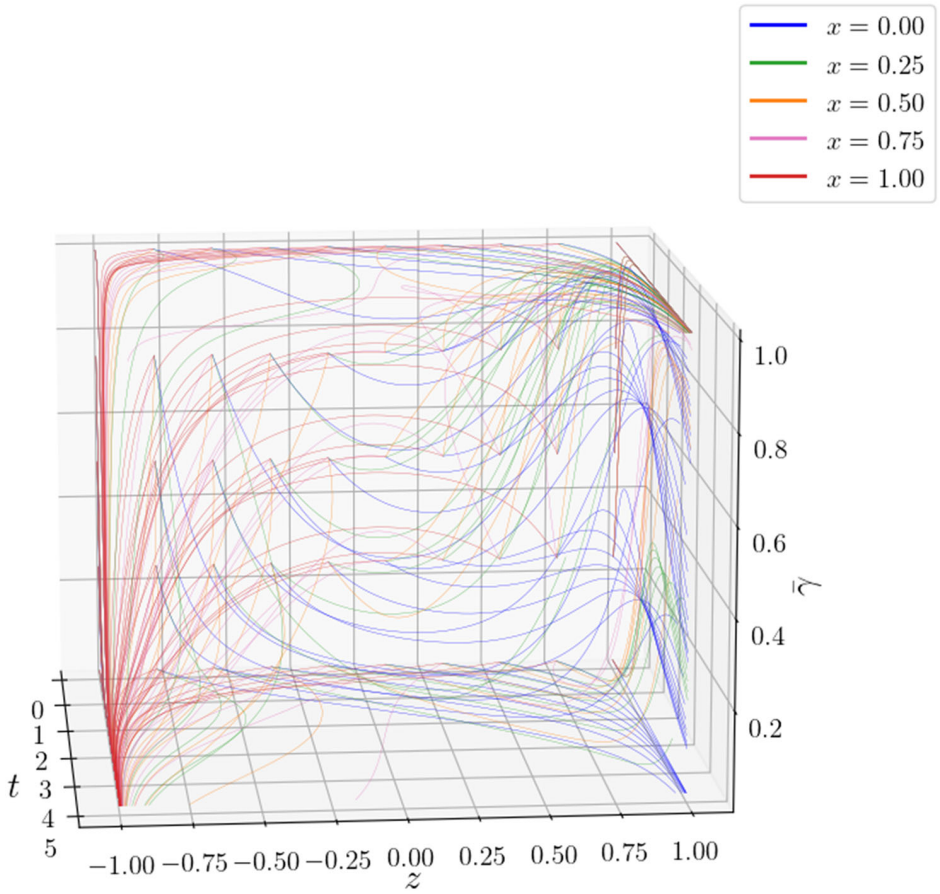

FIG. 3. Phase plots analyzing the role of initial conditions for the power-law model with $q = 1/2$. The other model parameters are set to $M = \Lambda = 10^{-4}$ and $\Omega_m = 0$. The colors of the trajectories indicate the initial value of x, as shown in the legend. It can be seen that trajectories with larger initial values of x end up at $z = -1$, whereas trajectories with smaller initial values of x end up at $z = 1$.

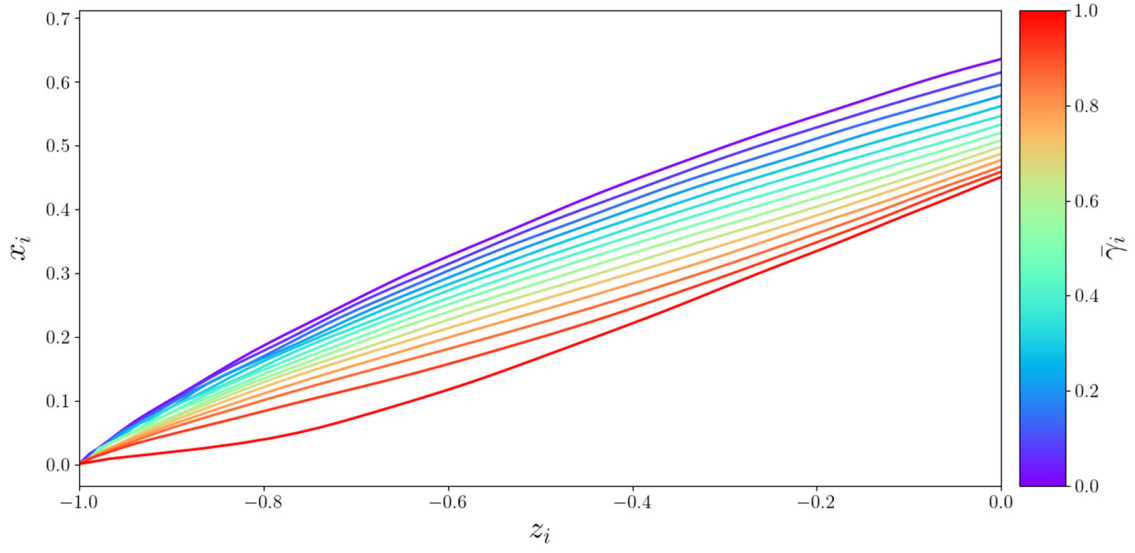

FIG. 4. Lines identify the maximum initial condition that results in an expanding universe, $z > 0$, with each color identified as the initial value of $\bar{\gamma}$, $\bar{\gamma}_i$. Therefore, the area under the line for each case of $\bar{\gamma}_i$ encodes the initial conditions that result in a bouncing scenario.

TABLE III. A table categorizing the stability of fixed points found by including a negative cosmological constant. We assume $0 < \Omega_C < 1$, disregarding any fixed results that set $\Omega_C = 0$ as this reduces back to Table I.

$\bar{\gamma}$	x	y	z	Existence	Stability
0	0	$\pm\sqrt{1-\Omega_m}$	$-\sqrt{\frac{2(\Omega_C-1)+3\Omega_m(1+w)}{-2+3(1+w_m)}}$	$\Omega_m(1+w_m) \geq \frac{2}{3}$	Stable
0	0	$\pm\sqrt{1-\Omega_m}$	$\sqrt{\frac{2(\Omega_C-1)+3\Omega_m(1+w_m)}{-2+3(1+w_m)}}$	$\Omega_m(1+w_m) \geq \frac{2}{3}$	Unstable
0	$\pm\sqrt{\frac{2(1-\Omega_C)-3\Omega_m(1+w_m)}{3}}$	$\sqrt{\frac{1+2\Omega_C+3\Omega_m w_m}{3}}$	0	$\Omega_m(1+w_m) \leq \frac{2}{3}(1-\Omega_C)$	Saddle
1	0	$\pm\sqrt{1-\Omega_m}$	$-\sqrt{\frac{2(\Omega_C-1)+3\Omega_m(1+w_m)}{-2+3(1+w_m)}}$	$\Omega_m(1+w_m) \geq \frac{2}{3}$	Stable
1	0	$\pm\sqrt{1-\Omega_m}$	$\sqrt{\frac{2(\Omega_C-1)+3\Omega_m(1+w_m)}{-2+3(1+w_m)}}$	$\Omega_m(1+w_m) \geq \frac{2}{3}$	Unstable
1	$\pm\sqrt{\frac{2(1-\Omega_C)-\Omega_m(1+w_m)}{6}}$	$\sqrt{\frac{4+2\Omega_C+3\Omega_m(w_m-1)}{6}}$	0	$\Omega_m(1+w_m) \leq 2(1-\Omega_C)$	Saddle
$\frac{1+w_m\Omega_m}{3(\Omega_m-1)}$	$\pm\sqrt{\frac{2(1-\Omega_C)-3\Omega_m(1+w_m)}{2-3\Omega_m(1+w_m)}}$	$\sqrt{\frac{2(1-\Omega_m)\Omega_C}{2-3\Omega_m(1+w_m)}}$	0	$w_m < 0, \Omega_m > \frac{1}{3}, \frac{2}{3} > \Omega_m(1+w_m)$	Unstable

We include a cosmological constant denoted by an energy density ρ_C (the equation of state is -1). The Friedmann equation becomes

$$3H^2 = \frac{\gamma^2\dot{\phi}^2}{\gamma+1} + V - 3\frac{K}{a^2} - \rho_C. \tag{37}$$

In the following we define the quantity $\tilde{D}^2 = H^2 + \frac{K}{a^2} + \frac{\rho_C}{3}$ in order to compactify the $K > 0$ state space. In addition, we define a new dimensionless variable $\Omega_C \equiv \frac{\rho_C}{3\tilde{D}^2}$. The only change to the equations of motion [Eqs. (20)–(23)] is

$$z' = (1-z^2)\left[1 - \frac{3}{2}x^2(1+\bar{\gamma})\right] - \Omega_C, \tag{38}$$

where $' \equiv \tilde{D}^{-1}\frac{d}{dt}$ as before, and the Friedmann constraint remains $x^2 + y^2 + \Omega_m = 1$. The same analysis can be performed by setting $w_m = -1$, which will remove Ω_m

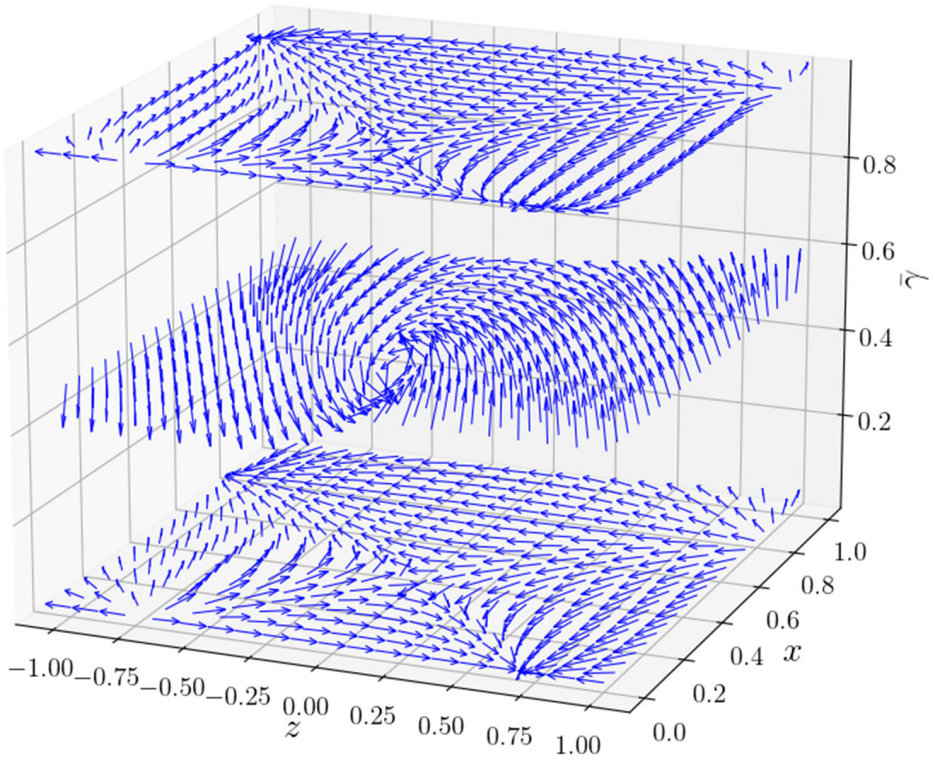

FIG. 5. Phase plots for the power-law model ($q = 1/2$) with a negative cosmological constant, set $\Omega_C = 0.3$. All other parameters are the same used to generate Fig. 2.

from Eqs. (20)–(23), giving the same results. We choose the equations above, as it provides an explicit dependence on Ω_C. We furthermore consider the power-law case with $q = 1/2$.

As shown in Fig. 5, the introduction of a negative cosmological constant leads to a noteworthy outcome—namely, an expansion in the range of larger "x" values that lead to a collapse, as compared to the scenario presented in Fig. 2. This expansion is attributed to the downward shift of the saddle point at $\bar{\gamma} = 0, 1$ concerning its x position, a change documented in Table I. Notably, the fixed points associated with $\bar{\gamma} = 0$ and $\bar{\gamma} = 1$ no longer display asymptotic quasi-de-Sitter solutions at $z = -1$ and $z = 1$, as shown in Fig. 5 and in Table III. However, this shift of the saddle point towards lower x values reduces the available parameter space conducive to a successful bounce scenario compared to the scenario discussed in Sec. III.

Our analysis results show that additional features or advantages emerge from including a negative cosmological constant. But we conclude that including a negative cosmological constant to the DBI model does not exhibit any further enhancement towards a cyclic model.

VIII. CONCLUSION

DBI models have generated significant interest due to their noncanonical kinetic term introduced by the brane, which results in a unique deceleration mechanism. This mechanism imposes a Lorentz factor that effectively sets a "speed limit" for the DBI scalar field, determined by the brane tension. This deceleration mechanism has led to many attractive inflationary models with unique potentials and nontrivial results. More recently, DBI models have been studied in the context of dark energy with interesting and future detectable features.

The authors of [29] conducted an in-depth dynamical analysis of a DBI field regarding dark energy and inflation, analyzing both exponential and power-law potentials and brane tensions. We have extended their analysis to include a closed universe, allowing us to explore the stability of additional fixed points, most interestingly around $z = 0$. Motivated by string theory phenomenology, we focused our numerical analysis on the power-law scenario, $V \propto \phi^2$ and $f \propto \phi^{-4}$.

From our analysis, we find the system is unstable in the regime $0 < \bar{\gamma} < 1$ and is driven to either the ultrarelativistic case, $\bar{\gamma} = 0$, or the conformal scalar field case, $\bar{\gamma} = 1$. This behavior is depicted in Fig. 2, where the regime $0 < \bar{\gamma} < 1$ drives the system to settle at the fixed points $\bar{\gamma} = 0$ or $\bar{\gamma} = 1$. The fixed point around $z = 0$ is a saddle in both the ultrarelativistic and conformal regimes. Although the system still accounts for a bouncing scenario, dependent on initial conditions, it lacks a generic cyclic behavior. We also find that including a DBI field increases the number of initial conditions that result in a bouncing universe, which reaches a maximum when $\bar{\gamma} = 0$. This result is depicted in Fig. 4, where we see that, given an ultrarelativistic case, the system has an increased number of initial conditions leading to a bounce compared to a conformally kinetic field.

Motivated by an increase in the initial conditions that allow for a successful bounce, we include an additional degree of freedom to induce a cyclic behavior. In Sec. VII, we investigate the effects of incorporating a negative cosmological constant into the analysis. While introducing a negative cosmological constant expands the range of points leading to collapse, the initial conditions that result in the bounce are constrained by the saddle point. Given a negative cosmological constant, it reduces the x value of the saddle fixed point. Therefore, in interest to this work, including a negative cosmological constant only reduces the initial conditions that lead to a bounce. Consequently, while a DBI field does lead to an increase of the initial conditions leading to a bounce, a more exotic degree of freedom is required to achieve a generic cyclic behavior.

ACKNOWLEDGMENTS

R. D. is supported by a STFC CDT studentship. P. K. S. D. thanks the First Rand Bank (SA) for financial support. M. C. is supported by the National Research Foundation (SA) Scarce-Skills Ph.D. Scholarship, and the University of Cape Town Science Faculty Ph.D. Scholarship.

[1] E. W. Kolb and M. S. Turner, *The Early Universe* (Taylor and Francis, Boca Raton, FL, 1990), Vol. 69.

[2] A. Macías and E. Castellanos, in *14th Marcel Grossmann Meeting on Recent Developments in Theoretical and Experimental General Relativity, Astrophysics, and Relativistic Field Theories* (World Scientific Publishing Co. Pte. Ltd., Singapore, 2017), Vol. 1, pp. 536–547.

[3] M. B. Green, J. H. Schwarz, and E. Witten, *Superstring Theory. Vol. 1: Introduction*, Cambridge Monographs on Mathematical Physics (Cambridge University Press, Cambridge, England, 1988).

[4] F. Marchesano, G. Shiu, and T. Weigand, arXiv:2401.01939.
[5] A. R. Liddle and D. H. Lyth, *Cosmological Inflation and Large Scale Structure* (Cambridge University Press, Cambridge, England, 2000).
[6] L. Amendola and S. Tsujikawa, *Dark Energy: Theory and Observations* (Cambridge University Press, Cambridge, England, 2015).
[7] S. Kachru, R. Kallosh, A. D. Linde, J. M. Maldacena, L. P. McAllister, and S. P. Trivedi, J. Cosmol. Astropart. Phys. 10 (2003) 013.
[8] M. Alishahiha, E. Silverstein, and D. Tong, Phys. Rev. D **70**, 123505 (2004).
[9] E. Silverstein and D. Tong, Phys. Rev. D **70**, 103505 (2004).
[10] C. Armendariz-Picon, T. Damour, and V. F. Mukhanov, Phys. Lett. B **458**, 209 (1999).
[11] J. Garriga and V. F. Mukhanov, Phys. Lett. B **458**, 219 (1999).
[12] S. Li and A. R. Liddle, J. Cosmol. Astropart. Phys. 10 (2012) 011.
[13] L. P. Chimento and R. Lazkoz, Gen. Relativ. Gravit. **40**, 2543 (2008).
[14] L. P. Chimento, R. Lazkoz, and M. G. Richarte, Phys. Rev. D **83**, 063505 (2011).
[15] W. H. Kinney and K. Tzirakis, Phys. Rev. D **77**, 103517 (2008).
[16] D. Bessada, W. H. Kinney, and K. Tzirakis, J. Cosmol. Astropart. Phys. 09 (2009) 031.
[17] S. Kecskemeti, J. Maiden, G. Shiu, and B. Underwood, J. High Energy Phys. 09 (2006) 076.
[18] M. Spalinski, J. Cosmol. Astropart. Phys. 05 (2007) 017.
[19] D. Langlois, S. Renaux-Petel, D. A. Steer, and T. Tanaka, Phys. Rev. D **78**, 063523 (2008).
[20] D. Langlois, S. Renaux-Petel, D. A. Steer, and T. Tanaka, Phys. Rev. Lett. **101**, 061301 (2008).
[21] X. Chen, Phys. Rev. D **72**, 123518 (2005).
[22] J. M. Weller, C. van de Bruck, and D. F. Mota, J. Cosmol. Astropart. Phys. 06 (2012) 002.
[23] M. X. Huang, G. Shiu, and B. Underwood, Phys. Rev. D **77**, 023511 (2008).
[24] J. Emery, G. Tasinato, and D. Wands, J. Cosmol. Astropart. Phys. 05 (2013) 021.
[25] C. Ahn, C. Kim, and E. V. Linder, Phys. Rev. D **80**, 123016 (2009).
[26] C. Ahn, C. Kim, and E. V. Linder, Phys. Lett. B **684**, 181 (2010).
[27] Z.-K. Guo and N. Ohta, J. Cosmol. Astropart. Phys. 04 (2008) 035.
[28] L. P. Chimento, R. Lazkoz, and I. Sendra, Gen. Relativ. Gravit. **42**, 1189 (2010).
[29] E. J. Copeland, S. Mizuno, and M. Shaeri, Phys. Rev. D **81**, 123501 (2010).
[30] B. Gumjudpai and J. Ward, Phys. Rev. D **80**, 023528 (2009).
[31] C. Kaeonikhom, D. Singleton, S. V. Sushkov, and N. Yongram, Phys. Rev. D **86**, 124049 (2012).
[32] E. Di Valentino, A. Melchiorri, and J. Silk, Nat. Astron. **4**, 196 (2019).
[33] W. Yang, W. Giarè, S. Pan, E. Di Valentino, A. Melchiorri, and J. Silk, Phys. Rev. D **107**, 063509 (2023).
[34] W. Handley, Phys. Rev. D **103**, L041301 (2021).
[35] R. Calderón, R. Gannouji, B. L'Huillier, and D. Polarski, Phys. Rev. D **103**, 023526 (2021).
[36] L. Visinelli, S. Vagnozzi, and U. Danielsson, Symmetry **11**, 1035 (2019).
[37] T. Biswas and A. Mazumdar, Phys. Rev. D **80**, 023519 (2009).
[38] F. Lucchin and S. Matarrese, Phys. Rev. D **32**, 1316 (1985).
[39] E. J. Copeland, A. R. Liddle, and D. Wands, Phys. Rev. D **57**, 4686 (1998).
[40] A. Paliathanasis, M. Tsamparlis, S. Basilakos, and J. D. Barrow, Phys. Rev. D **91**, 123535 (2015).
[41] E. J. Copeland, M. Sami, and S. Tsujikawa, Int. J. Mod. Phys. D **15**, 1753 (2006).